[19] H. Kirchhoff, "Wave propagation along radially inhomogeneous glass fibres," *Arch. Elektrische Übertragung*, vol. 27, pp. 13–18, Jan. 1973.
[20] G. L. Yip and S. Nemoto, "The relations between scalar modes in a lenslike medium and vector modes in a self-focusing optical fiber," *IEEE Trans. Microwave Theory Tech.*, vol. MTT-23, pp. 260–263, Feb. 1975.
[21] Y. Kokubun and K. Iga, "Mode analysis of graded-index optical fibers using a scalar wave equation including graded-index terms and direct numerical integration," *J. Opt. Soc. Amer.*, vol. 70, pp. 388–394, Apr. 1980.
[22] D. Gloge, "Weakly guiding fibers," *Appl. Opt.*, vol. 10, pp. 2252–2258, Oct. 1971.
[23] R. E. Collin, *Field Theory of Guided Waves*. New York: McGraw-Hill, 1960, p. 482.

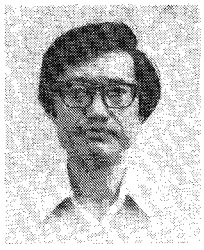

Nagayoshi Morita (M'67) was born in Toyama, Japan, on March 28, 1942. He received B.S., M.S., and Ph.D. degrees in engineering from Osaka University, Suita-shi, Japan, in 1964, 1966, and 1977, respectively.

Since 1966, he has been with the Department of Communication Engineering, Osaka University, Suita-shi, Japan, where he has been engaged in research work on discontinuities in millimeter waveguides and optical waveguides, analytic and numerical techniques for electromagnetic wave problems, bioelectromagnetics, etc.

Dr. Morita is a member of the Institute of Electronics and Communication Engineers of Japan, and Japan Society of Medical Electronics and Biological Engineering.

Refraction at a Curved Dielectric Interface: Geometrical Optics Solution

SHUNG-WU LEE, FELLOW, IEEE, MYSORE S. SHESHADRI, VAHRAZ JAMNEJAD, MEMBER, IEEE, AND RAJ MITTRA, FELLOW, IEEE

Abstract—**The transmission of a spherical or plane wave through an arbitrarily curved dielectric interface is solved by the geometrical optics theory. The transmitted field is proportional to the product of the conventional Fresnel's transmission coefficient and a divergence factor (DF), which describes the cross-sectional variation (convergence or divergence) of a ray pencil as the latter propagates in the transmitted region. The factor DF depends on the incident wavefront, the curvatures of the interface, and the relative indices of the two media. We give explicit matrix formulas for calculating DF, illustrate its physical significance via examples.**

I. Introduction

THE REFRACTION at a dielectric interface is of fundamental importance in electromagnetic theory. If the interface is arbitrarily curved, the only available solution is the one derived by the geometrical optics theory (GO). Such a solution consists of two main ingredients: the well-known Fresnel formulas for the transmission and reflection coefficients (due to A. J. Fresnel in 1823); and a so-called "divergence factor (DF)." Surprisingly, the solution of DF was derived as early as 1915 by Gullstrand [1], but its application was not widely recognized in the electromagnetic/optical community until very recently. In 1972, Deschamps [2], [3] rederived Gullstrand's result by using "curvature matrices" for describing curved surfaces/wavefronts, thus resulting in greater clarity and simpler computations.

In this paper, we supplement Deschamps' results by giving explicit formulas for calculating various curvature matrices and by illustrating the physical significance of DF via analytical and numerical examples. Another motivation for the present work is to compare our solution with the one described by Snyder and Love [4] for the same problem. It is shown that these two solutions are not in agreement.

II. Final Solution for the Refracted Fields

We begin with a statement of the problem. Two infinite dielectric media with refraction indices n_1 and n_2 are separated by a curved interface Σ (Fig. 1), which is described by

$$\Sigma: z = f(x, y). \tag{2.1}$$

The origin of the (x, y, z) coordinates is at the source point 0 in medium 1. The source emits a spherical wave, whose electric field at an observation point $\boldsymbol{r} = (r, \theta, \phi)$ is given by [for $\exp(j\omega t)$ time convention]

$$\boldsymbol{E}^i(\boldsymbol{r}) = \frac{e^{-jk_1 r}}{r}\left[\hat{\theta}P(\theta, \phi) + \hat{\phi}Q(\theta, \phi)\right] \tag{2.2}$$

Manuscript received March 23, 1981; revised July 30, 1981. This work was supported by the Naval Air Systems Command under Contract N00019-79-C-0281.

S. W. Lee, M. S. Sheshadri, and R. Mittra are with the Department of Electrical Engineering, University of Illinois, Urbana, IL 61801.

V. Jamnejad was with the Department of Electrical Engineering, University of Illinois, Urbana, IL 61801. He is now with Jet Propulsion Laboratory, Pasadena, CA 91103.

0018-9480/82/0100-0012$00.75 ©1982 IEEE

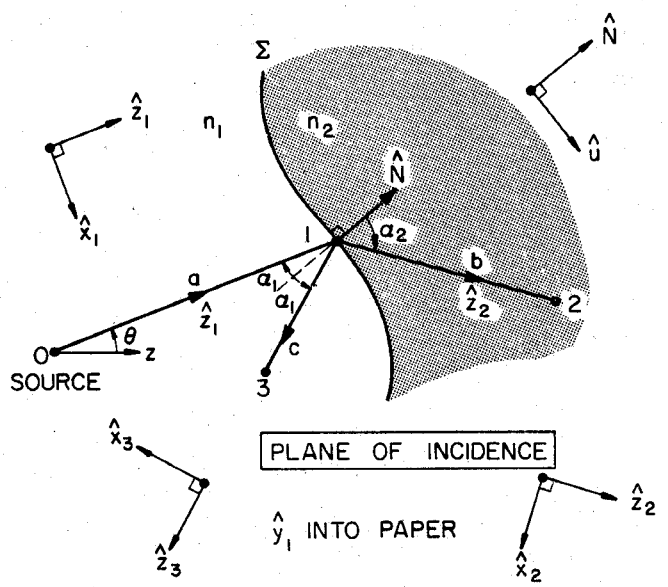

Fig. 1. Refraction at a curved dielectric interface Σ.

where $k_1 = 2\pi/\lambda_1 = n_1\omega/c$, and (r, θ, ϕ) are the spherical coordinates with origin at 0. The problem at hand is to find the transmitted field $\boldsymbol{E}^t$ at a typical point 2 in medium 2, and the reflected field $\boldsymbol{E}^r$ at a typical point 3 in medium 1.

We attack the problem by the GO [2], [3]. Referring to Fig. 1, let us concentrate on a typical incident ray in the direction of $\hat{z}_1$ emanating from the source at 0. The "outward" normal to surface Σ at the refraction point 1 is $\hat{N}$. The plane defined by the ray 01 and $\hat{N}$ is the plane of incidence. With respect to this plane, we resolve the incident field $\boldsymbol{E}^i$ into two components: perpendicular component $E^i_\perp$ and parallel component $E^i_\parallel$. We introduce a scalar u^i such that

$$u^i = \begin{cases} E^i_\perp, & \text{for perpendicular polarization} \\ H^i_\parallel, & \text{for parallel polarization.} \end{cases} \tag{2.3}$$

Similar decompositions and notations apply to $\boldsymbol{E}^t$ and $\boldsymbol{E}^r$. Then, the final solution derived from GO has the following form:

$$u^t(2) = (\mathrm{DF})_2 T e^{-jk_2 b} u^i(1) \tag{2.4a}$$

$$u^r(3) = (\mathrm{DF})_3 R e^{-jk_1 c} u^i(1) \tag{2.4b}$$

where b and c are the distances shown in Fig. 1 and the other factors in (2.4) are explained below. T and R are the well-known Fresnel's transmission and reflection coefficients (for a planar interface) given by

$$T = \frac{2}{1+Y} \qquad R = \frac{1-Y}{1+Y} \tag{2.5}$$

where

$$Y = \begin{cases} n(\cos\alpha_2/\cos\alpha_1), & \text{for perpendicular polarization} \\ n^{-1}(\cos\alpha_2/\cos\alpha_1), & \text{for parallel polarization} \end{cases}$$

$n = (n_2/n_1) =$ relative refraction index.

The incident angle α_1 and transmitted angle α_2 are related by the Snell's law

$$\sin\alpha_2 = \frac{1}{n}\sin\alpha_1 . \tag{2.6}$$

For $n < 1$, a critical incident angle α_c exists, where

$$\sin\alpha_c = n, \qquad \text{if } n < 1. \tag{2.7}$$

If $\alpha_1 > \alpha_c$, α_2 defined in (2.6) becomes complex, and the simple ray picture shown in Fig. 1 is lost. It is not immediately clear how the present GO solution must be modified. Therefore, in this paper, we exclude the case $\alpha_1 > \alpha_c$ when $n < 1$. (Discussion on this case can be found in [4] and [7].) The factor $(\mathrm{DF})_2$ in (2.4a) is the so-called "divergence factor" [3] of the transmitted ray pencil at point 2 in reference to point 1. It is given by

$$(\mathrm{DF})_2 = \frac{1}{\sqrt{1+(b/R_{21})}} \frac{1}{\sqrt{1+(b/R_{22})}} . \tag{2.8}$$

Here (R_{21}, R_{22}) are the two principal radii of curvature of the transmitted wavefront passing through point 1. The sign convention of R_{21} (or R_{22}) is as follows: R_{21} is positive if the transmitted rays in the corresponding normal section are divergent, and R_{21} is negative if the transmitted rays are convergent. The square roots in (2.8) take either positive real or negative imaginary value. Thus, $(\mathrm{DF})_2$ is positive real (no focus between points 1 and 2 on the transmitted ray), positive imaginary (one focus between 1 and 2), or negative real (two foci between 1 and 2). The factor $(\mathrm{DF})_3$ in (2.4b) is the divergence factor of the reflected ray pencil at point 3 in reference to point 1. It is given by

$$(\mathrm{DF})_3 = \frac{1}{\sqrt{1+(c/R_{31})}} \frac{1}{\sqrt{1+(c/R_{32})}} . \tag{2.9}$$

The determination of the four principal radii of curvature $(R_{21}, R_{22}, R_{31}, R_{32})$ is the key to the present problem. In Section III, we give an explicit, step-by-step description of their determination.

In summary, for the refraction problem in Fig. 1, the final solutions for the fields of the transmitted and reflected rays are given in (2.4). This solution is based on GO. It is valid for high frequencies, and for all cases, except when total reflection occurs ($n < 1$ and $\alpha_1 > \alpha_c$).

III. Calculation of Curvatures of Refracted Wavefronts

For an arbitrary interface Σ and an arbitrary incident ray 01 (Fig. 1), the calculation of the four radii of curvatures $(R_{21}, R_{22}, R_{31}, R_{32})$ is not a simple task. In this section, we present a systematic and explicit procedure for doing this calculation.

A. Coordinate Systems at Point 1

Consider a ray leaving the source at 0 in the direction (θ, ϕ), which intersects the surface Σ described in (2.1) at point 1. The distance a is determined from the nonlinear equation

$$a\cos\theta = f(x = a\sin\theta\cos\phi,\ y = a\sin\theta\sin\phi). \tag{3.1}$$

The unit vector in the direction of the incident ray is

$$\hat{z}_1 = \hat{x}\sin\theta\cos\phi + \hat{y}\sin\theta\sin\phi + \hat{z}\cos\theta. \quad (3.2)$$

The unit normal $\hat{N}$ of surface Σ at point 1 is

$$\hat{N} = \frac{1}{\Delta}(-f_x\hat{x} - f_y\hat{y} + \hat{z}) \quad (3.3)$$

where $\Delta = +(1+f_x^2+f_y^2)^{1/2}$, and f_x, for example, is the partial derivative of $f(x, y)$ with respect to x. By defining Δ positive, we have chosen $\hat{N}$ in the forward direction with respect to the incident ray. Vectors $\hat{z}_1$ and $\hat{N}$ define the plane of incidence. At point 1, we introduce four orthonormal base vectors: $(\hat{x}_1, \hat{y}_1, \hat{z}_1)$ for the incident ray 01; $(\hat{x}_2, \hat{y}_2, \hat{z}_2)$ for the transmitted ray 12; $(\hat{x}_3, \hat{y}_3, \hat{z}_3)$ for the reflected ray 13; $(\hat{u}, \hat{v}, \hat{N})$ for the surface Σ. We choose

$$\hat{y}_1 = \hat{y}_2 = \hat{y}_3 = \hat{v} = \hat{N}\times\hat{z}_1 \quad (3.4)$$

which is equal to a unit vector normal to the plane of incidence. Then it follows

$$\hat{u} = \hat{v}\times\hat{N} \qquad \hat{x}_n = \hat{y}_n\times\hat{z}_n, \qquad \text{for } n = 1,2,3. \quad (3.5)$$

The incident, transmitted, and reflected rays are respectively in the directions

$$\hat{z}_1 = \hat{u}\sin\alpha_1 + \hat{N}\cos\alpha_1 \quad (3.6a)$$

$$\hat{z}_2 = \hat{u}\sin\alpha_2 + \hat{N}\cos\alpha_2 \quad (3.6b)$$

$$\hat{z}_3 = \hat{u}\sin\alpha_1 - \hat{N}\cos\alpha_1 \quad (3.6c)$$

where

$$\sin\alpha_2 = n^{-1}\sin\alpha_1, \qquad 0 \leqslant \alpha_1, \qquad \alpha_2 \leqslant \pi/2. \quad (3.6d)$$

Note that, because of the particular choice in (3.4), both α_1 and α_2 are always positive, and have values in $(0, \pi/2)$.

B. Curvature Matrix of Surface Σ

At point 1 on surface Σ, the following two vectors lie in the tangent plane of the surface:

$$\boldsymbol{r}_{1x} = \hat{x} + f_x\hat{z} \qquad \boldsymbol{r}_{1y} = \hat{y} + f_y\hat{z} \quad (3.7)$$

where (x, y, z) are evaluated at point 1. With respect to the base vectors $(\boldsymbol{r}_{1x}, \boldsymbol{r}_{1y})$, the curvature matrix of Σ is given by [5]

$$\tilde{Q}_\Sigma = \frac{1}{\Delta^2}\begin{bmatrix} e_1G_1 - f_1F_1 & f_1E_1 - e_1F_1 \\ f_1G_1 - g_1F_1 & g_1E_1 - f_1F_1 \end{bmatrix} \quad (3.8)$$

where

$$\Delta = +\left(1+f_x^2+f_y^2\right)^{1/2}$$

$$E_1 = 1+f_x^2$$

$$F_1 = f_xf_y$$

$$G_1 = 1+f_y^2$$

$$e_1 = -\Delta^{-1}f_{xx}$$

$$f_1 = -\Delta^{-1}f_{xy}$$

$$g_1 = -\Delta^{-1}f_{yy}.$$

All (x, y, z)'s are evaluated at point 1. Now we transfer the curvature matrix with respect to $(\boldsymbol{r}_{1x}, \boldsymbol{r}_{1y})$ to that with respect to $(\hat{u}, \hat{v})$, namely

$$Q_\Sigma = A^{-1}\tilde{Q}_\Sigma A \quad (3.9)$$

where

$$A = \begin{bmatrix} \boldsymbol{r}_{1x}\cdot\hat{u} & \boldsymbol{r}_{1x}\cdot\hat{v} \\ \boldsymbol{r}_{1y}\cdot\hat{u} & \boldsymbol{r}_{1y}\cdot\hat{v} \end{bmatrix}.$$

It may be shown [5] that a principal radius calculated from (3.8) or (3.9) has a positive (negative) sign if the normal section of the surface bends away from (toward) the normal $\hat{N}$. For example, if Σ is a sphere with radius ρ and the normal $\hat{N}$ points away from the sphere center, we have

$$Q_\Sigma = \tilde{Q}_\Sigma = \rho^{-1}I \quad (3.10)$$

where I is the identity matrix. We note that the present sign convention for the surface curvature is the same as that used in [2], but opposite to that in [3], [5].

C. Curvature Matrices of Wavefronts

The incident wavefront passing through point 1 is spherical with a radius a. Thus, its curvature matrix Q_1 with respect to base vectors $(\hat{x}_1, \hat{y}_1)$, or any other orthonormal base vectors, is

$$Q_1 = a^{-1}I. \quad (3.11)$$

The curvature matrices of the transmitted and reflected wavefronts passing through 1 are expressed with respect to base vectors $(\hat{x}_2, \hat{y}_2)$, and $(\hat{x}_3, \hat{y}_3)$, respectively. They are denoted by Q_2 and Q_3. The solution of Q_2 is found from the following matrix equation [2]:

$$nB_2^TQ_2B_2 = B_1^TQ_1B_1 + (n\cos\alpha_2 - \cos\alpha_1)Q_\Sigma \quad (3.12)$$

where

$$B_n = \begin{bmatrix} \hat{x}_n\cdot\hat{u} & \hat{x}_n\cdot\hat{v} \\ \hat{y}_n\cdot\hat{u} & \hat{y}_n\cdot\hat{v} \end{bmatrix} = \begin{bmatrix} \cos\alpha_n & 0 \\ 0 & 1 \end{bmatrix}, \qquad n = 1,2.$$

The solution of Q_3 is found from the following matrix equation:

$$B_3^TQ_3B_3 = B_1^TQ_1B_1 - 2(\cos\alpha_1)Q_\Sigma \quad (3.13)$$

where

$$B_3 = \begin{bmatrix} \hat{x}_3\cdot\hat{u} & \hat{x}_3\cdot\hat{v} \\ \hat{y}_3\cdot\hat{u} & \hat{y}_3\cdot\hat{v} \end{bmatrix} = \begin{bmatrix} -\cos\alpha_1 & 0 \\ 0 & 1 \end{bmatrix}.$$

D. Principal Radii of Curvature of Refracted Wavefronts

Once matrices Q_2 and Q_3 are determined from (3.12) and (3.13), they may be diagonalized in a standard manner to find their eigenvectors (principal directions of the wavefront) and their eigenvalues (principal curvatures) [5]. In particular, the principal radii of the transmitted wavefront (R_{21}, R_{22}) are the roots of the following quadratic equation:

$$\frac{1}{R^2} - \frac{1}{R}(\text{trace } Q_2) + \det Q_2 = 0. \quad (3.14)$$

If Q_2 in (3.14) is replaced by Q_3, the two roots are the radii (R_{31}, R_{32}) of the reflected wavefront.

IV. Special Case: Spherical Interface

To illustrate the results obtained in the previous two sections, let us concentrate on a special case in which the interface Σ is spherical with radius $|\rho|$. Following our sign convention, the radius of curvature of Σ is

$$\rho = \begin{cases} +|\rho|, & \text{if } \Sigma \text{ is concave when viewed from the source} \\ -|\rho|, & \text{if } \Sigma \text{ is convex.} \end{cases} \tag{4.1}$$

Without loss of generality, we assume that the incident ray from the source at point 0 is in the direction $(\theta, \phi = 0)$. The plane of incidence is then the $x-z$ plane. Making use of the formulas in Section III, we find that the principal radii of the transmitted and reflected wavefronts passing through point 1 are

$$R_{21} = (n\cos^2\alpha_2)\left[\frac{1}{a}\cos^2\alpha_1 + \frac{1}{\rho}(n\cos\alpha_2 - \cos\alpha_1)\right]^{-1} \tag{4.2a}$$

$$R_{22} = \left[\frac{1}{na} + \frac{1}{n\rho}(n\cos\alpha_2 - \cos\alpha_1)\right]^{-1} \tag{4.2b}$$

$$R_{31} = \left[\frac{1}{a} - \frac{2}{\rho\cos\alpha_1}\right]^{-1} \qquad R_{32} = \left[\frac{1}{a} - \frac{2\cos\alpha_1}{\rho}\right]^{-1}. \tag{4.3}$$

It can be shown that R_{21} and R_{31} are the radii of curvature of the normal sections in the $x-z$ plane (plane of incidence), whereas R_{22} and R_{32} are those in the orthogonal directions. Since in general $R_{21} \neq R_{22}$ and $R_{31} \neq R_{32}$, the refracted and reflected pencils are astigmatic.

A. Normal Incidence

For $\alpha_1 = 0$, (4.2) and (4.3) become

$$R_{21} = R_{22} = n\left[\frac{1}{a} + \frac{n-1}{\rho}\right]^{-1}$$

$$R_{31} = R_{32} = \left[\frac{1}{a} - \frac{2}{\rho}\right]^{-1}. \tag{4.4}$$

Thus, for normal incidence, both refracted pencils have spherical wavefronts (no longer astigmatic). The relation in (4.4) may be rearranged to read

$$\frac{n}{R_{21}} = \frac{1}{a} + \frac{n-1}{\rho} \tag{4.5}$$

which is the well-known lens equation in optics. (See for example [6, eq. (40-14), p. 678].) Note the corresponding notations used in [6] and here: $n \to 1$, $n' \to n$, $s \to a$, $s' \to (-R_{21})$, and $R \to (-\rho)$.) The divergent incident pencil from a point source is converted into a convergent transmitted pencil in medium 2 when $R_{21} < 0$. This occurs when

$$a > \left(\frac{\rho}{1-n}\right) > 0. \tag{4.6}$$

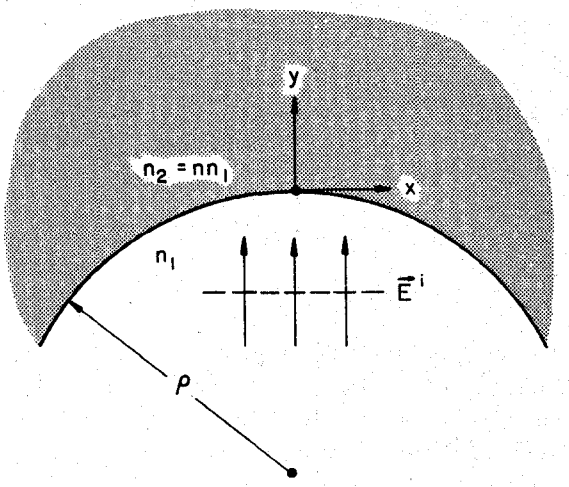

Fig. 2. Refraction at a concave spherical dielectric interface of a normally incident plane wave.

If $\rho > 0$ (concave dielectric interface), this is possible if $n = (n_2/n_1) < 1$. If $\rho < 0$ (convex dielectric interface), this is possible if $n > 1$.

B. Comparison with Snyder and Love's Result

In a recent article [4], Snyder and Love consider the problem sketched in Fig. 1 for an incident plane wave (source distance $a \to \infty$ in Fig. 1). Their final result is not in complete agreement with ours. To show this disagreement, let us concentrate on a simple case (Fig. 2): a concave, spherical, dielectric interface is illuminated by an incident plane wave which is given by

$$\boldsymbol{E}^i(x, y, z) = \hat{z}e^{-jk_1 y}. \tag{4.7}$$

The problem is to find the high-frequency solution of the refracted fields along the y-axis. Based on GO, our solution is given in (2.4), (2.5), (2.8), (2.9), and (4.4) with $a \to \infty$. Using the coordinate system in Fig. 2, the transmitted and reflected fields are

$$\boldsymbol{E}^t(0, y, 0) = \hat{z}\left[\frac{1}{1+\left(\frac{n-1}{n}\right)\left(\frac{y}{\rho}\right)}\right]\frac{2}{1+n}e^{-jk_2 y}, \qquad y > 0 \tag{4.8a}$$

and

$$\boldsymbol{E}^r(0, y, 0) = \hat{z}\left[\frac{1}{1-(2|y|/\rho)}\right]\frac{1-n}{1+n}e^{jk_1 y}, \qquad y < 0. \tag{4.8b}$$

The factors in [ ] in (4.8) are divergence factors. The intensity or power density of the incident field on the central ray (along $x = z = 0$) is given by

$$I^i = \mathrm{Re}\{\hat{y}\cdot(\boldsymbol{E}^i \times \boldsymbol{H}^{i*})\} = (n_1/120\pi), \qquad \mathrm{W/m^2} \tag{4.9}$$

which is independent of y since the incident field is a plane wave. The intensity of the refracted field on the central ray

does vary with y, namely

$$\frac{I^t(y)}{I^i}=n\left(\frac{2}{1+n}\right)^2\left[\frac{1}{1+\left(\frac{n-1}{n}\right)\left(\frac{y}{\rho}\right)}\right]^2, \qquad y>0 \tag{4.10a}$$

$$\frac{I^r(y)}{I^i}=\left(\frac{1-n}{1+n}\right)^2\left[\frac{1}{1-(2|y|/\rho)}\right]^2, \qquad y<0. \tag{4.10b}$$

At the focal point of the reflected pencil $y=-\rho/2$ in medium 1, the intensity I^r in (4.10b) predicted by the present GO becomes infinite as expected. For the same problem sketched in Fig. 2, Snyder and Love's solution is given in [4, eq. (29–34)]. For the case of normal incidence ($\alpha_i=0$) and central ray ($x=z=0$), Snyder and Love's solution reads

$$\boldsymbol{E}^i_{SL}(0,y,0)=\hat{z}\frac{2}{1+n}, \qquad \rho\gg y>0 \tag{4.11a}$$

$$\boldsymbol{E}^r_{SL}(0,y,0)=\hat{z}\frac{1-n}{1+n}e^{jk_1y}, \qquad y<0 \tag{4.11b}$$

which should be compared with our solution in (4.8). We note that i) divergence factors $(DF)_2$ and $(DF)_3$ are missing in (4.11), and ii) the propagation phase factor $\exp(-jk_2y)$ is missing in (4.11a). Thus, we believe that (4.11) is less accurate. Furthermore, for each incident ray (fixed α_i), Snyder and Love define a "power transmission coefficient T_{SL}" by [4, eq. (35a)]

$$T_{SL}=1-\left(\frac{I^r}{I^i}\right). \tag{4.12}$$

As may be seen from (4.10b), the intensity I^r is, in general, a function of position (x, y, z), because of the divergence/convergence of the reflected ray pencil. Then, T_{SL} when calculated correctly is also a function of position, and does not have the usual significance associated with the "power transmission coefficient."

V. Numerical Results and Discussions

For the refraction problem sketched in Fig. 1, the final solution for the transmitted field u^t in medium 2 is given in (2.4a), when the incident field is given in (2.2). In this section, we present some numerical results for u^t for various interfaces and source locations.

We consider three types of interfaces: the spherical interface described by

$$(z/\lambda_1)=1-\left[1-(x^2+y^2)/\lambda_1^2\right]^{1/2} \tag{5.1}$$

the paraboloidal interface described by

$$(z/\lambda_1)=(x^2+y^2)/2\lambda_1^2 \tag{5.2}$$

and the hyperboloidal interface described by

$$(z/\lambda_1)=\tfrac{1}{2}\left[1+2(x^2+y^2)/\lambda_1^2\right]^{1/2}-\tfrac{1}{2} \tag{5.3}$$

where λ_1 is the wavelength in medium 1 in which the source is located. For easy comparison, we have chosen the above interfaces such that they all have the same curvature in the axial direction. The source is assumed to be y-polarized. We calculate the transmitted field in the E-plane (plane normal to $\hat{x}$) and H-plane (plane normal to $\hat{y}$). In these two planes, the incident field is assumed to be

$$\boldsymbol{E}^i(r)=\frac{e^{-jk_1r}}{r}\begin{cases}\hat{\theta}1, & E\text{-plane}\\ \hat{y}1, & H\text{-plane.}\end{cases} \tag{5.4}$$

Thus, in the E-plane, the $\boldsymbol{E}$-vector is parallel to the plane of incidence; whereas in the H-plane, the $\boldsymbol{E}$-vector is perpendicular. The observation point 2 is in medium 2 (Fig. 1) with distance $b\to\infty$ (far zone). We calculate the normalized far field defined by

$$EN=\left|\frac{\boldsymbol{E}^t(2)}{\boldsymbol{E}^i(2)}\right|=\left|\frac{E\text{-field when } n_1\neq n_2}{E\text{-field when } n_1=n_2}\right|. \tag{5.5}$$

Substitute (2.4a) and (5.4) into (5.5). Under the condition $b\to\infty$, we have

$$EN\sim\frac{1}{a}T\sqrt{R_{21}R_{22}}, \qquad b\to\infty. \tag{5.6}$$

Here a is the distance between the source and the interface along the incident ray, and T is the Fresnel's transmission coefficient given in (2.5). The factor $\sqrt{R_{21}R_{22}}$ is the radius of the Gaussian curvature. In presenting the numerical results, we plot EN as a function of θ, where θ is the polar angle of observation point 2 measured from a line parallel to the z-axis and passing through the source points. The relative index $n=n_2/n_1$ is always set at 2 (transmission into a denser medium).

A. Concave Spherical Interface

Figs. 3 and 4 show the E- and H-plane far-field pattern EN as a function of θ. Note that the field strengths increase as the source moves closer to the interface (smaller a) because EN is inversely proportional to a, according to (5.5). The Gaussian curvature $\sqrt{R_{21}R_{22}}$ decreases with a, but not enough to offset the factor $(1/a)$ in (5.5). For source 3, which is at the center of the spherical interface, all of the incident rays are normal to the interface. It can be shown that $R_{21}=R_{22}=a$. Thus, EN calculated from (5.5) is equal to T, which is 0.667 for the present case of $n=2$. Of particular interest is the H-plane pattern of source 1 shown in Fig. 4. Note the marked asymmetry in the far-field pattern which is due to the asymmetry of the surface with respect to source 1. Fig. 5 shows the variation of the axial far field when the source is moved along and parallel to the z-axis. It shows clearly the increase of the field as the source moves closer to the interface.

B. Concave Hyperboloidal Interface (Fig. 6)

Note that the far-field pattern (due to source 4) has a dip instead of a peak in the axial direction. This is in the contrast to the situations in Figs. 3 and 4. There is another fact worth mentioning. Because of the choice of the same axial curvature for the above interfaces, the axial field is the same for both interfaces when the source is at 2, 3, or 4.

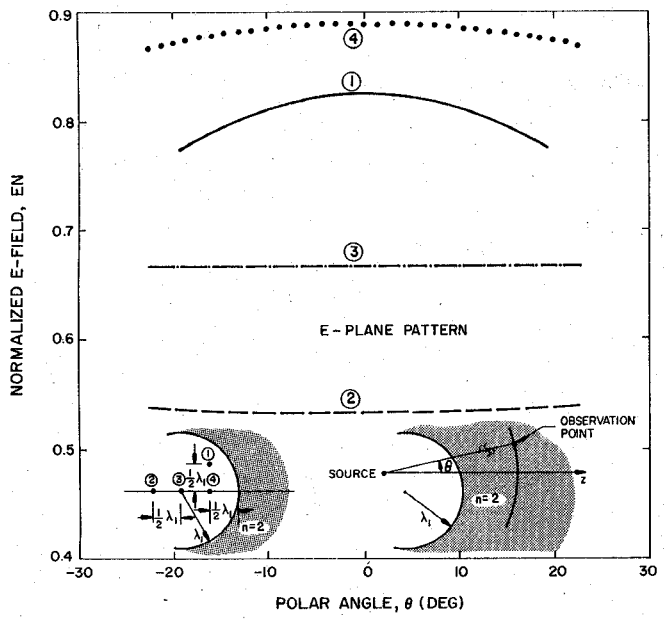

Fig. 3. *E*-plane far-field pattern through a concave spherical interface. The isotropic source is located at ①, ②, ③, and ④.

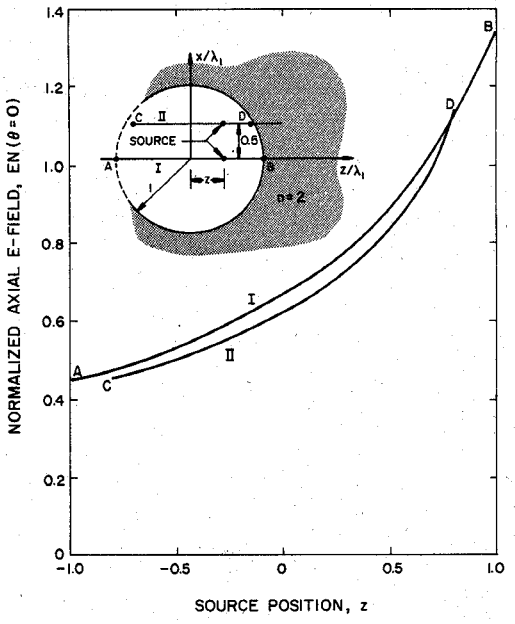

Fig. 5. Axial far-field variation with source position for a concave spherical interface.

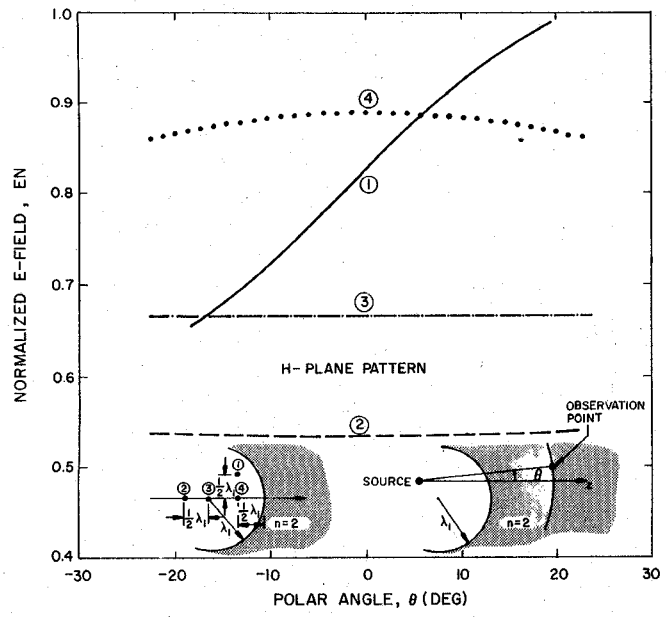

Fig. 4. Same as Fig. 3, except for *H*-plane pattern.

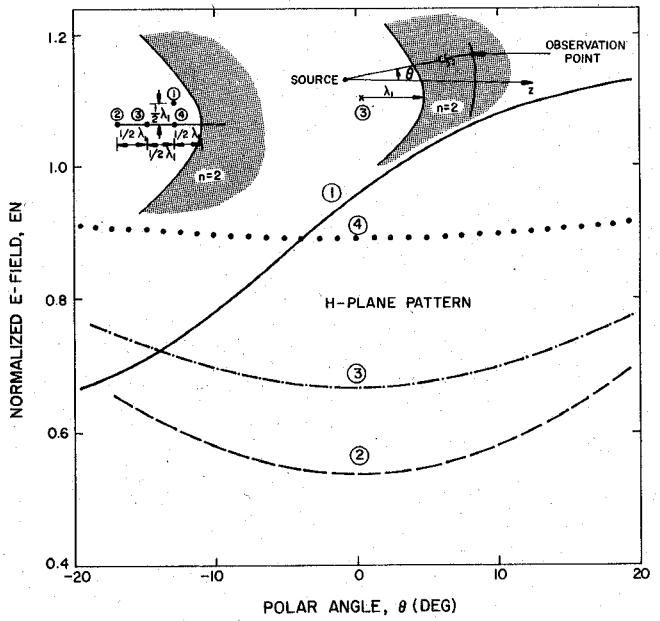

Fig. 6. *H*-plane far-field pattern through a concave hyperboloid.

However, for source 1, which is displaced from the symmetry axis, the normalized axial field $EN(\theta=0)$ increases from 0.826 for the spherical surface to 0.954 for the hyperboloid.

C. Convex Interfaces

The *H*-plane far-field patterns for a convex sphere, paraboloid and hyperboloid are shown in Fig. 7 for source locations 5 and 6. The source locations 5 and 6 were chosen based on (4.6). Source 5 produces a divergent axial pencil in medium 2, whereas source 6 produces a convergent axial pencil; the behavior in the nonaxial direction is governed by the type of the interface. Thus, as may be seen from Fig. 7, the far field in the axial direction through the spherical interface has a peak for source 6 and a dip for source 5. This is also the case for the paraboloid. However, this behavior is not observed in the hyperboloidal pattern.

For all the convex interfaces, the variation of EN as a function of θ in (5.5) is predominantly determined by the radius of the Gaussian curvature, $\sqrt{R_{21}R_{22}}$, and to a lesser extent by T or a.

D. Ray Picture

The *H*-plane pattern due to source 6 for a convex sphere is given in Fig. 7. The corresponding ray picture is shown in Fig. 8. We launch 6 rays at 4° apart in the upper half

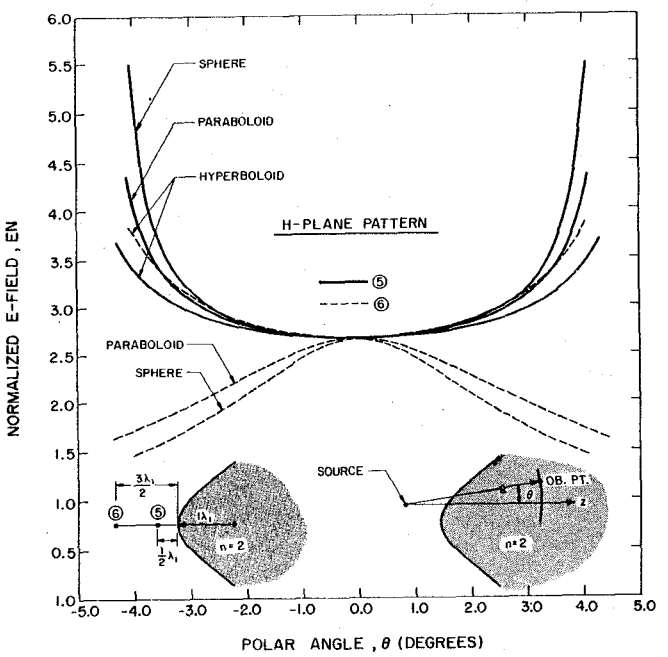

Fig. 7. *H*-plane far-field pattern through convex interfaces.

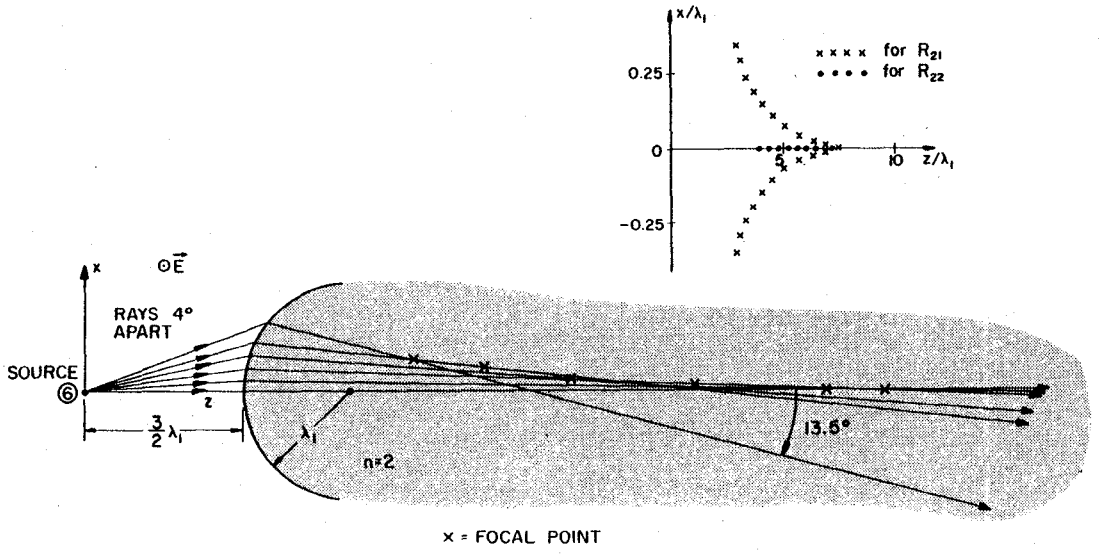

Fig. 8. Ray picture and trace of foci of the transmitted rays which lie in the $x-z$ plane, for the convex spherical interface with source at ⑥. The distance from the interface to a cross along a given ray represents R_{21}.

$x-z$ plane ($x>0$). The transmitted rays are first convergent, and after crossing the caustic surface, become divergent. The incident rays in the upper half $x-z$ plane within a 20° angle give rise to transmitted rays in the *lower* $x-z$ plane ($x<0$) within a 13.5° angle. There are two caustic surfaces associated with the transmitted rays. The intersections of the caustic surfaces and the $x-z$ plane are indicated by crosses and dots. Similar ray pictures can be drawn for the other cases also.

VI. Conclusion

For the refraction problem sketched in Fig. 1, the final geometrical-optics solutions for the transmitted field and the reflected field are given in (2.4). They are applicable under rather general conditions, namely, the dielectric interface described in (2.1) is arbitrary, and the incident field in (2.2) from a point source is arbitrary. A major step in calculating these solutions is the evaluation of the divergence factors in (2.8) and (2.9), which involves the matrix operation described by (3.12) and (3.13). Strictly speaking, the present solution is valid in the high-frequency limit $\omega \to \infty$; however, practical experience has shown that solutions of the present type are reasonably accurate as long as the radii of curvature of the dielectric interface are in the order of a wavelength or more.

References

[1] A. Gullstrand, "Das allgemeine optische Abbildungs system Svenska Vetensk," *Handl.*, vol. 55, pp. 1–139, 1915.

[2] G. A. Deschamps, "Ray techniques in electromagnetics," *Proc. IEEE*, vol. 60, no. 9, pp. 1022–1035, Sept. 1972.

[3] S. W. Lee, "Geometrical theory of diffraction in electromagnetics, Vol. 1: Geometrical optics," University of Illinois, Urbana, IL, Electromagnetics Lab. Rep. 78-2, 1978.
[4] A. W. Snyder and J. D. Love, "Reflection at curved dielectric interface—electromagnetic tunneling," *IEEE Trans. Microwave Theory Tech.*, vol. MTT-23, pp. 134–141, 1975.
[5] S. W. Lee, "Differential geometry for GTD applications," University of Illinois, Urbana, IL, Electromagnetics Lab. Rep. 77-21, 1977.
[6] F. W. Sears, M. W. Zemansky, and H. D. Young, *University Physics*. 5th ed., Reading, MA: Addison-Wesley, 1976.
[7] D. S. Jones, "Electromagnetic tunneling," *Quart J. Mech. Appl. Math.*, vol. 31, part 4, pp. 409–434, Nov. 1978.

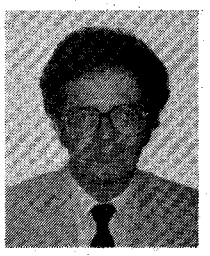

Vahraz Jamnejad (M'79) was born in Tehran, Iran, in 1945. He received the B.S. degree in electrical engineering from Tehran University in 1967 and the M.S. and Ph.D. degrees from the University of Illinois, Urbana, in 1971 and 1974, respectively.

He was a Research Associate with the Electromagnetics Laboratory of the University of Illinois during the year 1974–1975 and joined the Technical University of Tehran (formerly Arya-Mehr) in 1975 as an Assistant Professor. He was a Visiting Assistant Professor at the University of Illinois where he was affiliated with the Electromagnetics Laboratory during 1978–1979. Presently he is a Member of the technical staff of the Jet Propulsion Laboratory of the California Institute of Technology, Pasadena. His areas of research include antennas, electromagnetic scattering and diffraction, microwaves, millimeter waves, and computer techniques. Presently he is involved in research and development in the area of satellite antenna systems.

Dr. Jamnejad is a member of Phi Kappa Phi.

Shung-Wu Lee (S'63–M'66–SM'73–F'81) was born in Kiangsi, China. He recieved the M.S. and Ph.D. degrees in electrical engineering from the University of Illinois, Urbana, in 1964 and 1966, respectively.

He is currently an Associate Professor at the University of Illinois. In 1968 he received the Everett Award for excellence in undergraduate teaching. During the summers of 1966 through 1970 he was a member of the Technical Staff of the Hughes Aircraft Company, Fullerton, CA. As a recipient of an NSF NATO Fellowship in 1973, he was a Guest Lecturer at the Technical University, Eindhoven, The Netherlands, and the University of London, England.

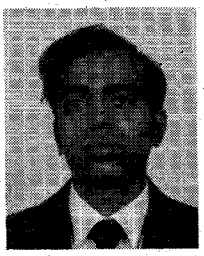

Mysore S. Sheshadri received the B.E. degree in electronics engineering from the Bangalore University, Bangalore, India, in 1972 and the Masters degree in microwave and radar engineering from the Indian Institute of Technology, Kharagpur, India, in 1975. In 1976 he was awarded a fellowship by the Council of Scientific and Industrial Research, India, to pursue the Ph.D. degree at the Indian Institute of Technology, Madras. He received the Ph.D. degree in 1978.

From 1972 to 1973 he was with Bharath Electronics, Ltd., Bangalore, as an Assistant Engineer, working on radar systems. During 1978–1979 he was with the Indian Space Research Organization, Bangalore, engaged in the development and testing of communications satellites. He is presently with the Electromagnetics Laboratory of the University of Illinois, Urbana. His current research interests include the design of shaped reflectors and the application of geometrical optics to the analysis of radomes.

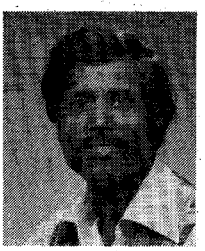

Raj Mittra (S'54–M'57–SM'69–F'71) is Professor of electrical engineering and Associate Director of the Electromagnetics Laboratory at the University of Illinois in Urbana. He serves as a Consultant to several industrial and governmental organizations, including the NASA Jet Propulsion Laboratory of the California Institute of Technology.

His professional interests include the areas of analytical and computerated electromagnetics, satellite antennas, integrated circuits, coherent optics, transient problems, radar scattering, and so on. He is Past-President of AP-S, currently serves as an Editor of AP-S TRANSACTIONS and is an active contributor to the many activities of the Society.